Check for updates

Electrochemical sensor based on amine- and thiol-modified multi-walled carbon nanotubes for sensitive and selective determination of uranyl ions in real water samples†

Amina A. Selim,[a] A. B. Abdallah, [iD] *[ab] Fathi S. Awad, [iD] *[ab] Magdi E. Khalifa[a] and Ahmed Fathi Salem Molouk [iD] [ab]

Novel selective and sensitive electrochemical sensors based on the modification of a carbon paste electrode (CPE) with novel amine- and thiol-functionalized multi-walled carbon nanotubes (MWCNT) have been developed for the detection and monitoring of uranyl ions in different real water samples. Multiwalled carbon nanotubes were grafted with 2-aminothiazole (AT/MWCNT) and melamine thiourea (MT/MWCNT) *via* an amidation reaction in the presence of dicyclohexyl carbodiimide (DCC) as a coupling agent. This modification for multiwalled carbon nanotubes has never been reported before. The amine and thiol groups were considered to be promising functional groups due to their high affinity toward coordination with uranyl ions. The modified multi-walled carbon nanotubes were characterized using different analytical techniques including FTIR, SEM, XPS, and elemental analysis. Subsequently, 10 wt% MT/MWCNT was mixed with 60 wt% graphite powder in the presence of 30 wt% paraffin oil to obtain a modified carbon paste electrode (MT/MWCNT/CPE). The electrochemical behavior and applications of the prepared sensors were examined using cyclic voltammetry, differential pulse anodic stripping voltammetry, and electrochemical impedance spectroscopy. The MT/MWCNT/CPE sensor exhibited a good linearity for UO_2^{2+} in the concentration range of 5.0×10^{-3} to 1.0×10^{-10} mol L^{-1} with low limits of detection (LOD = 2.1×10^{-11} mol L^{-1}) and quantification (LOQ = 7×10^{-11} mol L^{-1}). In addition, high precision (RSD = 2.7%), good reproducibility (RSD = 2.1%), and high stability (six weeks) were displayed. Finally, MT-MWCNT@CPE was successfully utilized to measure the uranyl ions in an actual water sample with excellent recoveries (97.8–99.3%). These results demonstrate that MT-MWCNT@CPE possesses appropriate accuracy and is appropriate for environmental applications.

1. Introduction

Uranium is one of the most abundant hazardous actinide metals, and has a radioactive nature. However, it is widely utilized as a primary source of energy and is widely applied in various fields, including nuclear power stations, military applications such as nuclear weapons,[1] and medicine. It is worth mentioning that long-term exposure to uranyl causes adverse effects to human health, such as kidney failure, chemical changes in bones,[2,3] lung cancer, genetic diseases, and urinary[4] and digestive system ailments. Thus, there is an urgent

need to monitor the concentration of uranyl ions using a simple and sensitive technique.

To date, various analytical approaches, including atomic absorption spectrometry (AAS),[5,6] gas chromatography (GC),[7] inductively coupled plasma mass spectroscopy (ICP-MS),[8] and X-ray fluorescence spectrometry (XRF),[9,10] have been employed for the analysis of uranyl ions. These methods are time-consuming, expensive, and require expensive instrumentation and trained staff. Electroanalytical methods are powerful tools that have been exploited for heavy metal ion detection over the years owing to their fast response times, ease of use, and good controllability. Notably, the direct electrochemical determination of uranyl ions in conventional glassy carbon and metal electrodes still suffers from obstacles, such as weak output signals and low sensitivity and selectivity over time, which could be attributed to surface fouling and passivation. Synthetic efforts have been exerted by scholars to develop the sensitivity and selectivity of the working electrode surface. Significant improvements in electrode sensing have been reported using

[a]Chemistry Department, Faculty of Science, Mansoura University, Mansoura 35516, Egypt. E-mail: fathyawad949@yahoo.com; ahmed.bahgat@mans.edu.eg; Tel: +201000166374; +201090433272

[b]Chemistry Department, Faculty of Science, New Mansoura University, New Mansoura City, Egypt

† Electronic supplementary information (ESI) available. See DOI: https://doi.org/10.1039/d3ra05374a

conducting polymers,[11,12] metal nanoparticles,[13,14] Ni/NiO partially oxidized carbon nanomaterials,[15] graphene oxide,[11,16] and multi-walled carbon nanotubes (MWCNT).[17] Among these, MWCNT, a rising star on the horizon of materials science, are excellent candidates for sensor fabrication because of their unique physiochemical properties, large surface area, high electrical conductivity, and fast electron transfer kinetics.[18–25] Additionally, sensitivity can be enhanced dramatically by using alternative voltammetric techniques, especially differential pulse stripping voltammetry (DPSV).[26–28] The DPSV technique is one of the most sensitive approaches, owing to the deposition of all target metal ions on the electrode surface at a high negative potential. The deposited metal is stripped in the opposite direction, and the electrochemical signals are recorded.[26–28] To date, only Zhu *et al.* have employed the DPSV technique for the detection of uranyl ions using a glassy carbon electrode (GCE), which was modified by cupferron and diphenyl guanidine.[27] Although this assay has good selectivity, it also suffers from many shortcomings, including a poor linear range (3–80 μg L^{-1}) and the moderate stability of the modified GCE.[27]

Thus, this study aims to fabricate a new electrochemical sensor based on a carbon paste electrode modified with pristine and modified MWCNT for uranyl ion detection depending on the DPSV. This work reports the chemical modification of multiwalled carbon nanotubes by functionalization with melamine-based chelating ligands and 2-aminothiazole ligands for the effective and selective sensing of UO_2^{2+} from water sources. The melamine-thiourea-modified multiwalled carbon nanotubes (MT/MWCNT) combine the heavier donor atom sulfur with the amine and triazine nitrogen functional groups attached to the carboxylated multiwalled carbon nanotubes to effectively capture UO_2^{2+} from water. Additionally, introducing ligands containing donor atoms such as sulfur will increase the capacity of melamine toward heavy metals, since its electron cloud can be easily polarized because it has a large size and nearly full d-electrons.[29] Additionally, the Lewis-base groups of melamine thiourea and aminothiazole donate their lone pair electrons to the Lewis-acid empty d orbitals of the UO_2(II) ions to form stable complexes. The MWCNT were first oxidized and then modified with 2-aminothiazole (AT) and/or the melamine thiourea ligand (MT ligand). The synthesized samples were characterized using Fourier transform infrared (FTIR) spectroscopy, scanning electron microscopy (SEM), transmission electron microscopy (TEM), X-ray diffraction (XRD), and X-ray photoelectron spectroscopy (XPS). Subsequently, they were mixed with graphene powder in the presence of paraffin oil. Various parameters (*e.g.*, pH, deposition potential, and deposition time) affecting the efficiency of the appropriate sensor response were investigated. Subsequently, under the optimized conditions, the developed sensor was successfully applied for the determination of uranyl in different real samples using the DPSV technique.

2. Experimental section

For more details on the materials and instruments, see ESI S1 and S2,† respectively.

2.1. Synthesis of amine- and thiol-modified multi-walled carbon nanotubes

To increase the number of carboxylic groups on the surface of multi-walled carbon nanotubes, MWCNT (0.5 g) were suspended in 10 mL of a mixture of concentrated nitric acid (68.0 ± 0.5% v/v) and water with a ratio of (1 : 1) under sonication for 30 min and then refluxed at 120 °C for 12 h. The final material (O-MWCNT) was centrifuged, washed with distilled water several times, and dried for 12 h at 80 °C.

The prepared O-MWCNT were modified with melamine thiourea or 2-aminothiazole *via* an amidation reaction between the free amine groups in 2-aminothiazole or melamine thiourea and the carboxyl (COOH) groups of the oxidized multi-walled carbon nanotubes in the presence of *N,N'*-dicyclohexylcarbodiimide (DCC) as a coupling agent. This procedure was adapted from our previous work with slight modifications. Typically, 0.3 g of the O-MWCNT was dispersed in 20 mL of anhydrous DMF using sonication for 30 min. Subsequently, 2-aminothiazole (AT) or melamine thiourea (MT; prepared as described in our previous work)[29,30] was added in excess (0.5 g), and 1.0 g of *N,N'*-dicyclohexylcarbodiimide (DCC) (Sigma-Aldrich, 99.0%) was added. After that, the mixture was refluxed at 90 °C for 10 h. The mixture was then centrifuged, and the solid material was washed with DMF, ethanol, and distilled water. The final product was then dried for 12 h at 80 °C. The general procedure for the synthesis of the modified multi-walled carbon nanotubes is illustrated in Scheme 1.

2.2. Electrochemical measurements

To study the electrochemical behavior of the proposed sensors, a bare CPE or modified CPE was connected to a calomel electrode and platinum wire and then immersed in a solution containing 5×10^{-3} mol L^{-1} UO_2^{2+} buffered with acetate (pH 2). Subsequently, the CV data were recorded. Additionally, using the DPSV technique, the electrochemical detection of uranyl ions was performed under the optimized conditions (scanning voltage: −0.2–1 V; step size: 5 mV; pulse size: 100 mV). All electrochemical measurements were performed at room temperature after purging the electrochemical solution with nitrogen gas. For EIS measurements, these electrodes were inserted in a 0.1 mol L^{-1} potassium chloride solution with 5 mmol L^{-1} $Fe(CN)_6^{3-/4-}$ as the redox-active probe.

2.3. Actual sample analysis

To evaluate the potential practical use and efficiency of the developed sensor, it was important to use MT-MWCNT@CPE for the determination of uranyl in real water samples. Water samples were collected from the Baltim Sea (Baltim, Egypt). Filter paper was used to filter the water samples and remove solid contaminants. Subsequently, for electrochemical sensing, differential pulse anodic stripping voltammetry (DPASV) was applied to 30 mL of the water sample containing 3 mL of pH 2 buffer to measure the concentration of uranyl. Standard solutions of uranyl were added to the resulting water samples.
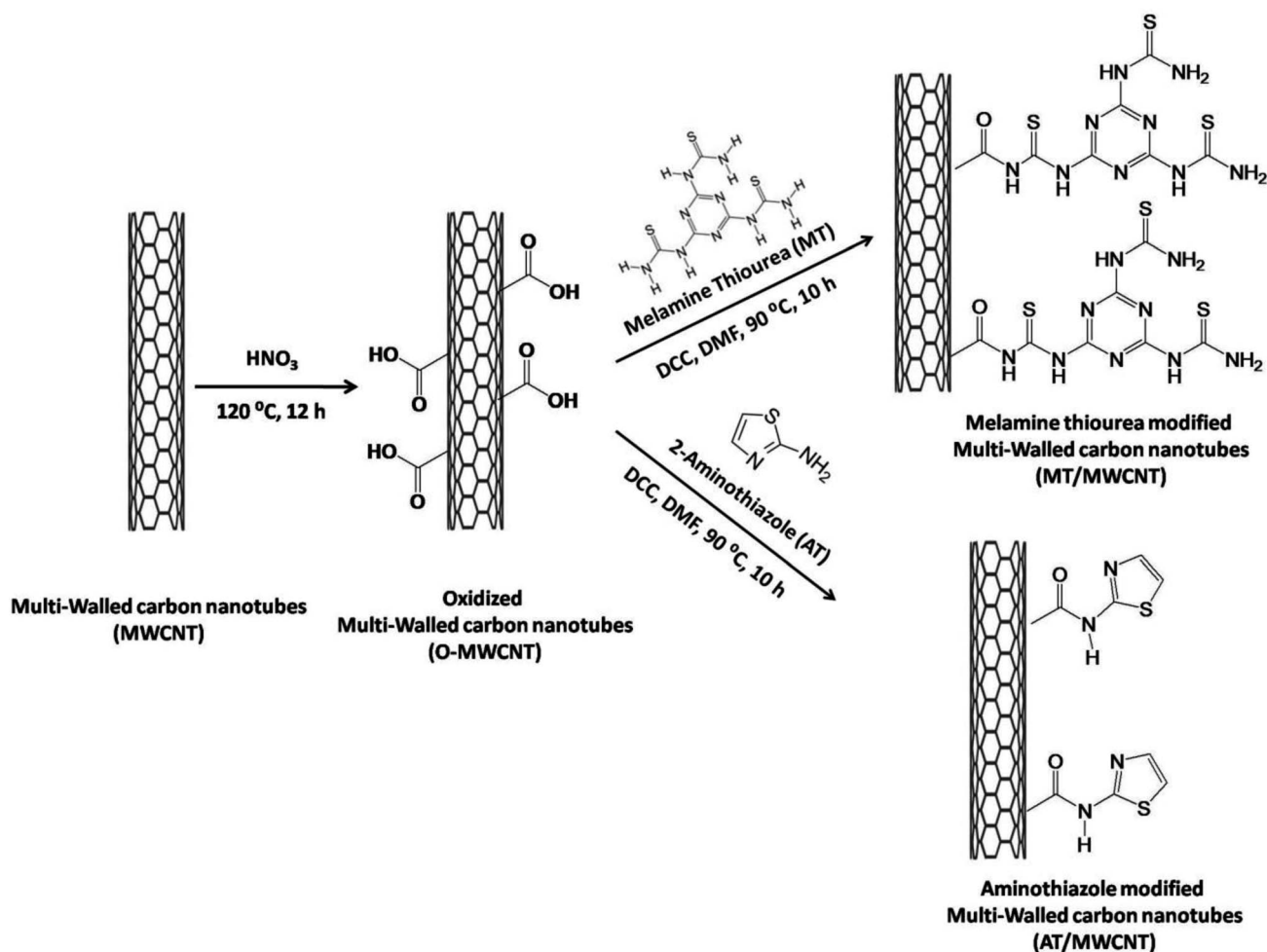
Scheme 1 General procedure for the preparation of AT/MWCNT and MT/MWCNT.

3. Results and discussion

3.1. Characterization of 2-aminothiazole-modified carbon nanotubes (AT/MWCNT) and melamine-thiourea-modified carbon nanotubes (MT/MWCNT)

The AT/MWCNT and MT/MWCNT composites were characterized using various analytical techniques. FTIR analysis was conducted to confirm the successful incorporation of amine and thiol groups onto the surface of the multi-walled carbon nanotubes upon chemical functionalization with the active ligands 2-aminothiazole or melamine thiourea (Fig. 1). The FTIR spectra of melamine thiourea and 2-aminothiazole exhibited peaks in the region 3087–3400 cm^{-1} and at 1640 cm^{-1} related to the N–H stretching and bending oscillations, respectively (Fig. S1†). The peaks at 1021 cm^{-1} and 578 cm^{-1} were ascribed to the triazine ring vibrations.[31,32] Additionally, the peaks between 1433–1533 cm^{-1} and at 810 cm^{-1} can be attributed to the stretching and bending vibrations of C–N. Two distinguished peaks at 1620 and 2046 cm^{-1} were also observed, corresponding to the bending and stretching oscillations of C=S, respectively. As shown in Fig. S1,† two new peaks at 692 cm^{-1} and 1173 cm^{-1} corresponding to C–S bending and stretching

oscillations were observed in the melamine thiourea and 2-aminothiazole spectra.[31,32] The FTIR spectra of the pristine multi-walled carbon nanotubes (MWCNT) show peaks at 3451, 1638, and 1070 cm^{-1}, which are related to the stretching vibrations of O–H, C=C (in aromatic rings), and C–O, respectively[33,34] As shown in Fig. 1, significant changes in the spectrum of the multi-walled carbon nanotubes occur upon oxidation with nitric acid to form O-MWCNT. A new peak at 1729 cm^{-1} corresponding to the C=O stretching vibrations of carboxylic groups is clearly observed.[35] The sharp peak observed at 1384 cm^{-1} was attributed to the bending vibrations of hydroxyl group C–O–H.[36] Thus, the number of carboxyl groups on the surface of the multi-walled carbon nanotubes was enhanced upon oxidation with nitric acid.

Comparing the spectrum of the O-MWCNT with that of the MT/MWCNT or AT/MWCNT, the C=O stretching vibration of the COOH group in the O-MWCNT disappears, and new peaks are clearly observed at 1626 and 1573 cm^{-1}, which can be assigned to the C=O stretching vibration of the NHCO (amide) and the bending vibrations of N–H in the NH$_2$ group, respectively.[29,30,37] Furthermore, the band at 3328 cm^{-1} (in the AT/ MWCNT) and 3455 cm^{-1} (MT/MWCNT) can be assigned to
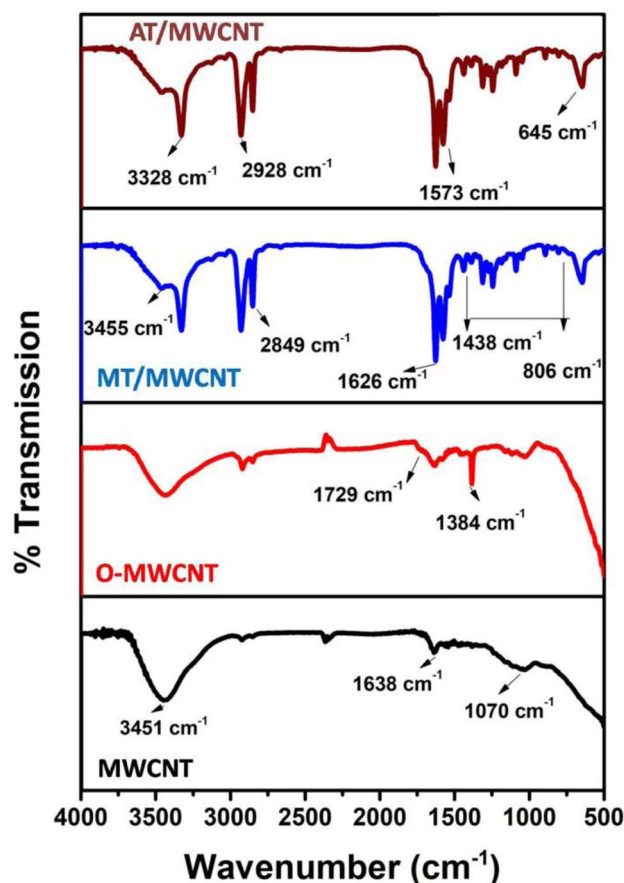
Fig. 1 FTIR spectra of MWCNT, O-MWCNT, AT/MWCNT, and MT/MWCNT.

the N–H stretching vibration of the secondary amine.[29,37,38] Also, new peaks are observed in the MT/MWCNT spectrum at 1240–1320, 1090, and 645 cm^{-1}, which were assigned to C–N stretching vibrations (triazine), –C=S vibrations, and C–S vibrations, respectively.[29,35,38] These results indicate the successful functionalization of the surface of the multiwalled carbon nanotubes with melamine thiourea or aminothiazole chelating ligands through amide linkage (peptide linkage).

XPS analysis was used to investigate the surface elements of the MWCNT upon functionalization with the melamine thiourea active ligand. The XPS survey results for MWCNT and MT/MWCNT are displayed in Fig. S2.† Two peaks related to C 1s and O 1s were observed for the MWCNT and MT/MWCNT. In addition, two new peaks corresponding to N 1s and S 2p were present in the MT/MWCNT spectrum. Furthermore, Table S1† demonstrates that the N content increased from 0.2% to 13.51% and the S content increased from 0.2 to 1.2% after the modification of MWCNT with melamine thiourea.

The C 1s XPS spectrum of MT/MWCNT (Fig. 2A) revealed three peaks at 284.0 eV (C in C–C and C=C), 285.0 eV (C in C–N and C–S), and 287.78 eV (C in N–C=O, C=N, C=S).[39] The high-resolution O 1s spectrum of MT/MWCNT (Fig. 2B) reveals two peaks with binding energies of 531.18 eV (O in O–H) and 532.18 eV (O in C=O).[37] Detailed N 1s and S 2p XPS

measurements of MT/MWCNT confirmed the successful grafting of melamine thiourea onto the surface of MWCNT 29–30. The high-resolution N 1s spectrum (Fig. 2C) revealed two peaks at 399.18 eV (N in N–C=O) and 379.98 (N in C–N–C and C=N).[40] The high resolution S 2p spectrum (Fig. 2D) can be deconvoluted into three peaks, two at 164.16 eV (S 2p$_{3/2}$) and 165.2 (S 2p$_{1/2}$) attributed to the sulfur binding in –C–S or S–H bonds and conjugated –C=S– bonds, and at 168.7 eV related to the oxidized sulfur (C–SO$_X$).[29,30]

The MWCNT, O-MWCNT, AT/MWCNT, and MT/MWCNT morphologies were investigated using scanning electron microscopy (SEM). As shown in Fig. 3A, the MWCNT displayed an entangled tubular structure, which increased the surface area. As seen in Fig. 3B, the O-MWCNT resembles a thread-like network with slight fragmentation, which indicates that the MWCNT are shortened after oxidation treatment.[41] After chemical functionalization with 2-aminothiazole or melamine thiourea, the O-MWCNT became coarser. Additionally, the entangled tubes disappeared and the surface became crowded with regular particles (Fig. 3C and D). This significant change in the morphology reflects the successful grafting of the active ligands AT and MT onto the surface of the MWCNT, which increases the number of active sites with a high affinity for uranyl ions. Additionally, SEM images with EDX analysis of the AT/MWCNT and MT/MWCNT are displayed in Fig. S3.† The EDX analysis (Fig. S3†) clearly shows the presence of N and S in addition to C and O in the AT/MWCNT and MT/MWCNT, which provide evidence for the incorporation of amine and thiol groups onto the MWCNT surface.

3.2. Electrochemical measurements

3.2.1. Cyclic voltammetry. The electrochemical performance of the synthesized sensors (CPE, MWCNT/CPE, oxidized MWCNT/CPE, AT/MWCNT/CPE, and MT/MWCNT/CPE) was estimated using CV and electrochemical impedance spectroscopy (EIS) in uranyl solution. Preliminary investigations revealed the appearance of a new distinct signal for uranyl ions in acetate buffer when compared with acetate buffer only using a bare CPE (Fig. S4†). Thus, CV was carried out in 20 mL of uranyl acetate solution (5×10^{-3} mol L^{-1}) containing 3 mL of buffer (pH 2) as a supporting electrolyte, as shown in Fig. 4. Compared to that of the bare CPE, the electrochemical behavior of the modified electrode MWCNT/CPE was enhanced, which might be attributed to its large surface area and faster electron transfer. Notably, the electrochemical signals increased slightly after the oxidation of the surface of the MWCNT. To improve the sensitivity of the modified MWCNT@CPE, the carbon nanotubes were modified with melamine thiourea (MT) or 2-aminothiazole (AT). The anodic peak current of the MT/MWCNT/CPE gradually rose. These results may be due to the presence of the different functional groups in the melamine thiourea, which can easily react with and capture the target uranyl ions.

3.2.2. Electrochemical impedance study. Electrochemical impedance spectroscopy measurements were performed under the optimized conditions (AC amplitude: 10 mV, frequency: 0.1–
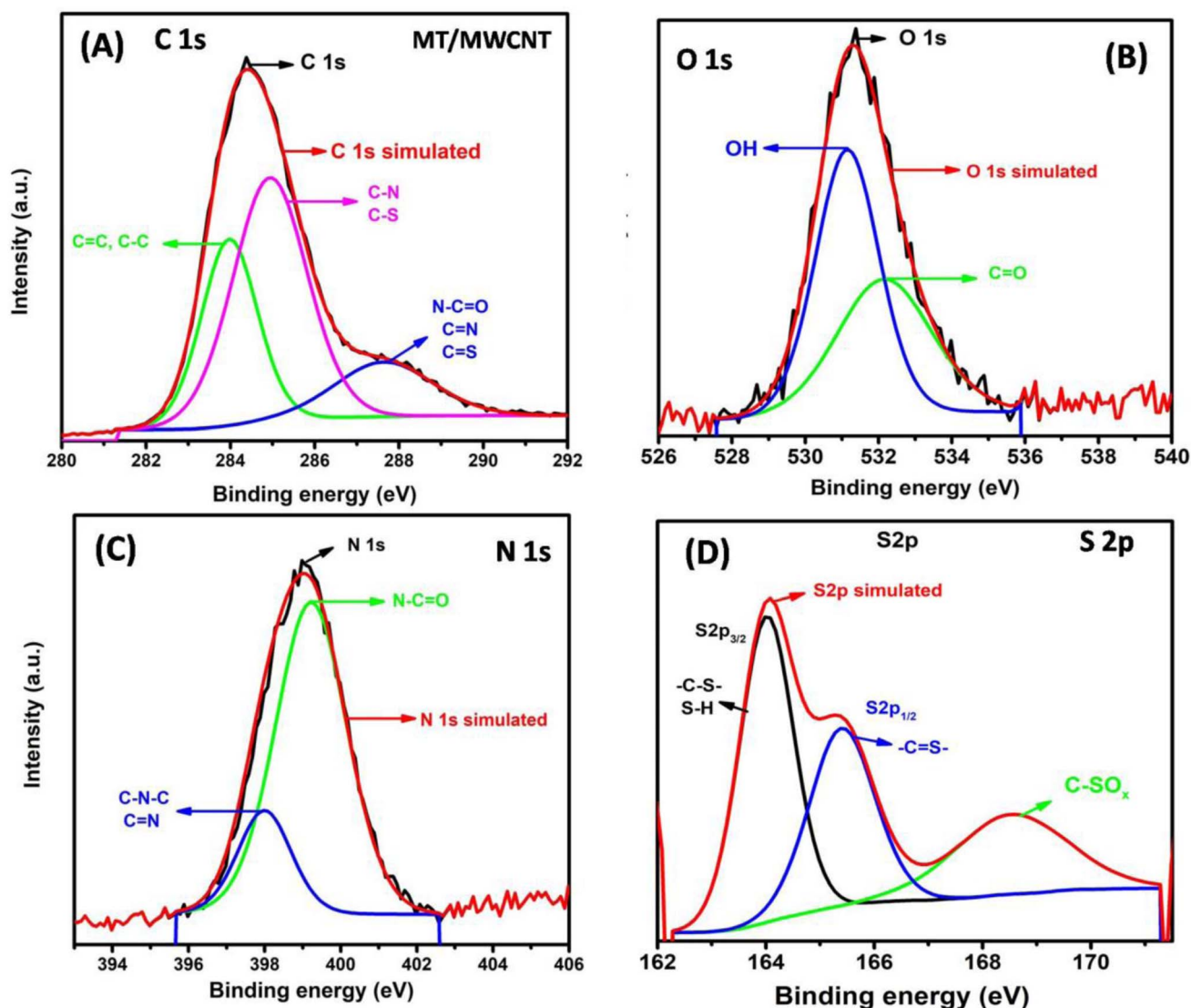
Fig. 2   XPS high-resolution spectra of C 1s (A), O 1s (B), N 1s (C), and S 2p (D) in MT/MWCNT.

10^{-5} Hz, open circuit: 0.1 V) in a solution containing 0.1 mol L^{-1} potassium chloride solution and 5 mmol L^{-1} Fe(CN)$_6^{3-/4-}$ as the supporting electrolyte solution. As exhibited in Fig. 5, the charge transfer resistance (R_{ct}) decreased after the modification of the bare CPE ($R_{ct} = 820\ \Omega\ cm^2$) with the MWCNT and/or oxidized MWCNT ($R_{ct} = 730\ \Omega\ cm^2$), which may be attributed to the high surface area and electrical conductivity of the MWCNT after modification of the MWCNT with the MT.

The charge transfer resistances (R_{ct}) for both MT-MWCNT and AT-MWCNT were estimated based on fitting using the depicted equivalent circuit.[42] The R_{ct} was measured from the difference between the low-frequency and high-frequency intercepts on the real axes for the fitted arc.[42] The resulting values of R_{ct} for MT-MWCNT and AT-MWCNT were 660 Ω cm^2 and 830 Ω cm^2, respectively. R_{ct} decreased sharply again in MT/MWCNT/CPE because of the presence of the different functional groups of the MT ligand, which enhanced electron transfer. It is worth mentioning that the data obtained from the

electrochemical impedance measurements are similar to the CV results.

3.2.3. Effect of pH. The hydrogen ion concentration has a significant effect on the electrochemical determination of uranyl ions. Therefore, the influence of pH in the range of 2–8 was evaluated using acetate and phosphate buffers. As shown in Fig. S5,† a high electrochemical response was observed for MT/MWCNT/CPE at pH 2. These results may be due to the presence of UO$_2^{2+}$ ions, which are common species that tend to be easily reduced and deposited on the modified electrode surface. A low peak current was observed at high pH values, which could be attributed to the formation of UO$_2$Ac$^+$, UO$_2$(Ac)$_2$, and UO$_2$(Ac)$_3^-$. Therefore, a pH of 2 was chosen for uranyl determination.

3.2.4. Effect of scan rate. To study the electrochemical mechanism of the reaction process at MT/MWCNT/CPE, the electrochemical reaction was measured in 5.0 $\times$ 10^{-3} mol L^{-1} uranyl at pH 2 at different scan rates. As shown in Fig. S6A,† the anodic currents increased linearly with the square root of the
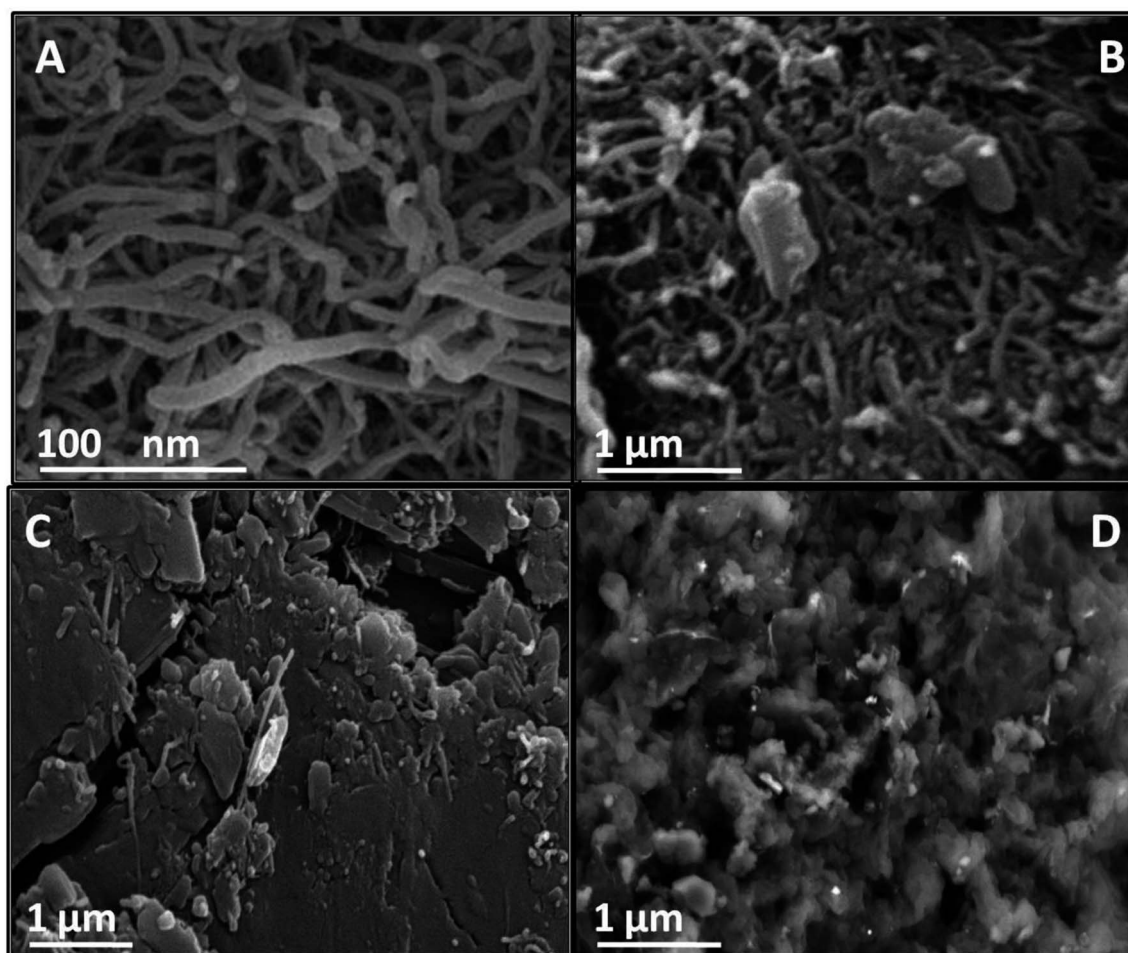
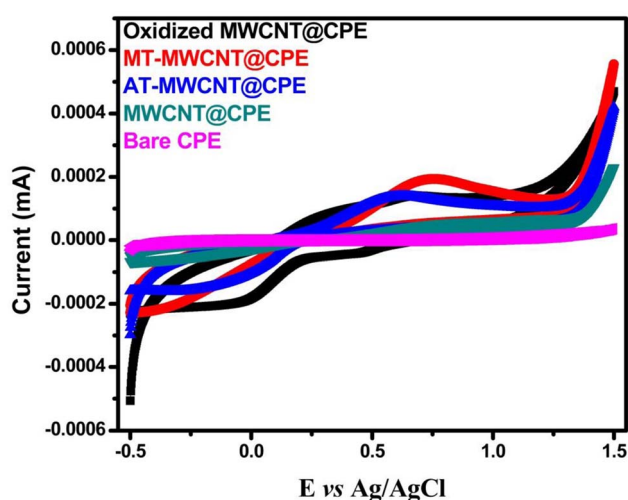**Fig. 3** SEM images of MWCNT (A), O-MWCNT (B), MT/MWCNT (C), and AT/MWCNT (D).

Fig. 4 Cyclic voltammograms of CPE, MWCNT/CPE, oxidized MWCNT/CPE, AT/MWCNT/CPE, and MT/MWCNT/CPE in 5×10^{-3} mol L^{-1} UO$_2^{2+}$ solution buffered with acetate (pH 2).

scan rate, which emphasized that the diffusion process controlled the electrochemical reaction. In contrast, the anodic potential gradually increased with the logarithm of the scan rate

(Fig. S5B†). In addition, the number of electrons in the electrochemical reaction was calculated using the Tafel equation, and was equal to 2.

3.2.5. Deposition potential and deposition time. The deposition step significantly improved the sensitivity of the DPASV method. The deposition potential is typically related to the standard reduction potential, at which the uranyl ions are reduced on the modified CPE sensor to concentrate them at the electrode surface. Thus, different deposition potentials in the range from −700 to 1500 mV were tested. As presented in Fig. 6A, high peak current signals were observed at 1400 mV. Furthermore, the deposition time was examined in the range of 20–150 s, and the anodic response increased gradually and reached a high response at 90 s, which enables all the ions to be pre-concentrated at the MT/MWCNT/CPE surface (Fig. 6B).

3.2.6. Leaching process and time. To improve the sensitivity of this technique, the pre-concentrated uranyl ions at the MT/MWCNT/CPE should be leached from the electrode surface after each measurement. Sodium hydroxide, hydrochloric acid, methanol, and methanol containing different ratios of acetic acid were tested for uranyl removal after the determination process. Complete removal of uranyl ions was achieved using
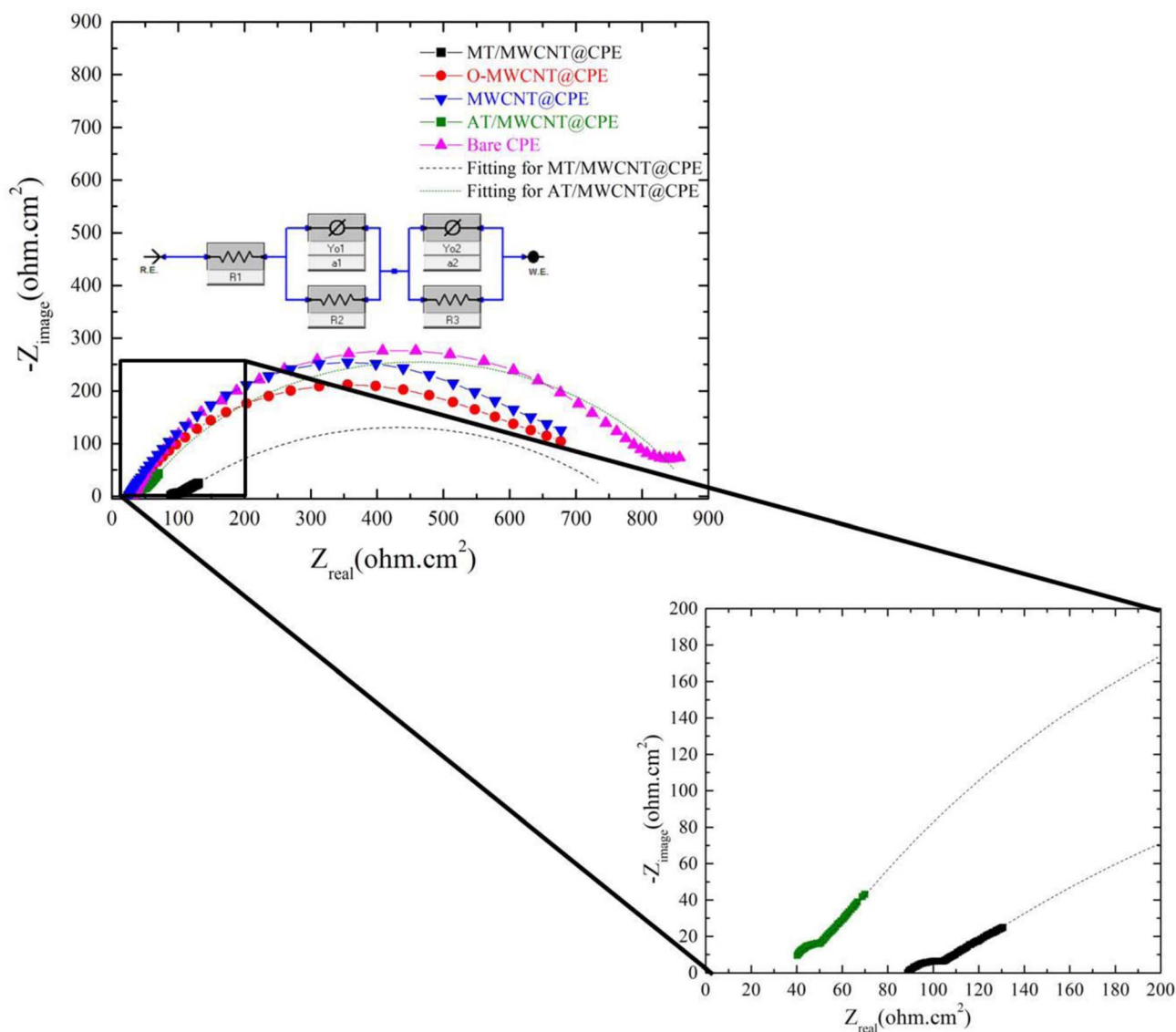
Fig. 5 EIS of CPE, MWCNT/CPE, O-MWCNT/CPE, AT/MWCNT/CPE, and MT/MWCNT/CPE in a solution of 5 mmol L^{-1} Fe(CN)$_6^{3-/4-}$ and 0.1 mol L^{-1} KCl.
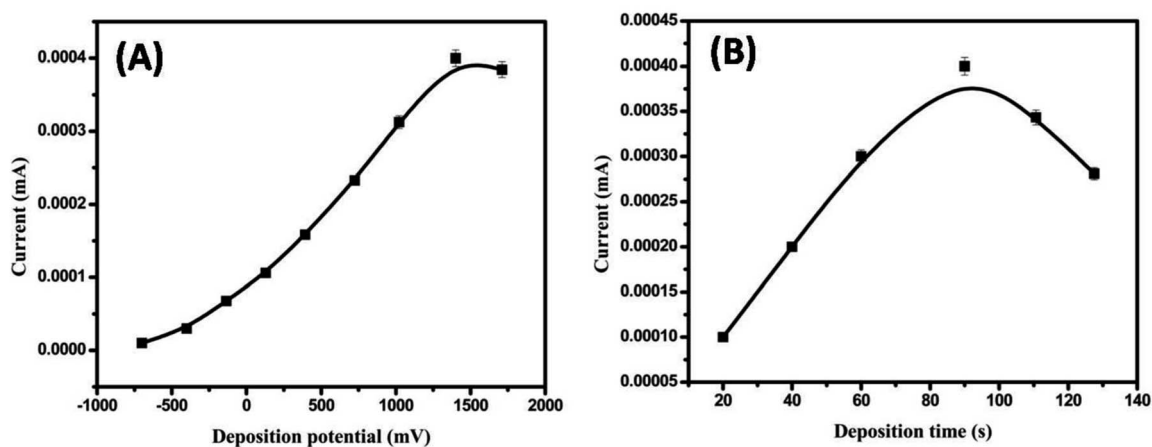

Fig. 6 Effect of (A) deposition potential (deposition time; 90 s, scan rate: 100 mV s^{-1}; pulse amplitude: 50 mV; pulse width: 50 ms) and (B) deposition time on the stripping peak current of 5×10^{-3} mol L^{-1} UO_2^{2+} solution buffered with pH 2 acetate (deposition potential; 1400 mV, scan rate; 100 mV s^{-1}; pulse amplitude: 50 mV; pulse width: 50 ms).
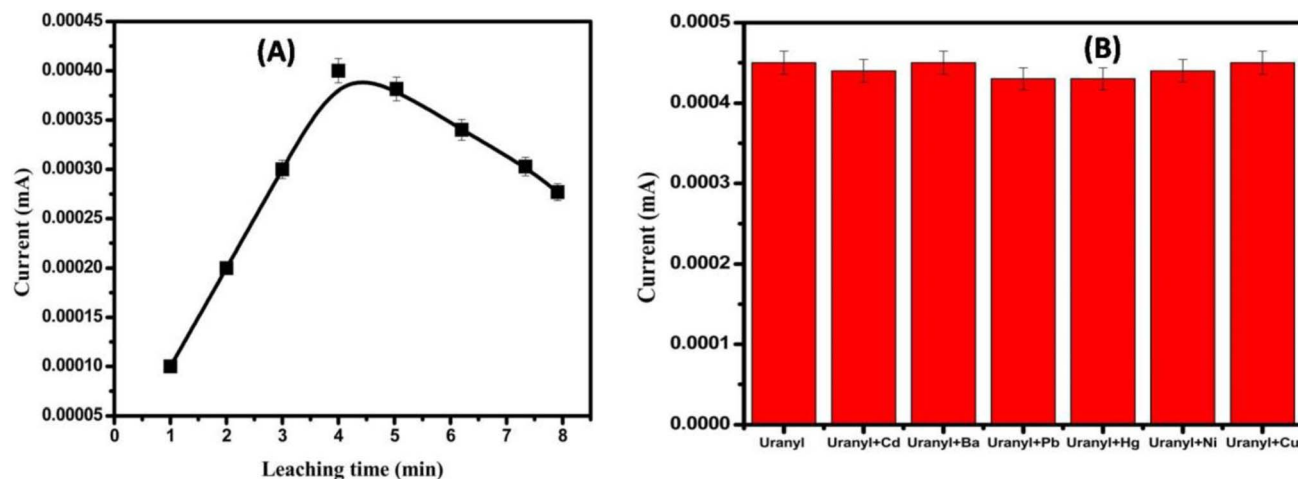
Fig. 7 (A) Effect of leaching time of MT/MWCNT@CPE on the anodic stripping peak current. (B) Selectivity of MT/MWCNT@CPE for UO_2^{2+} detection in the presence of the interfering ions Cd^{2+}, Ba^{2+}, Pb^{2+}, Hg^{2+}, Ni^{2+}, Cu^{2+} (10^{-3} mol L^{-1}).
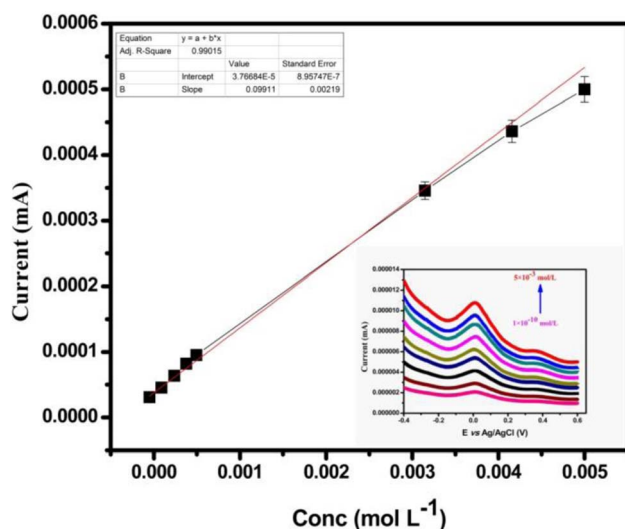

Fig. 8 Oxidation peak current of MT-MWCNT@CPE in different ranges of concentrations of UO_2^{2+}; deposition potential: 1400 mV.

hydrochloric acid (0.01 mol L^{-1}). Furthermore, anodic signals were recorded over a period of 1–8 min. As shown in Fig. 7A, 4 min was the optimal leaching time.

3.2.7. Interference studies. For the electrochemical sensors, the selectivity toward uranyl ions was evaluated by introducing a series of various foreign metal ions, namely, Cd^{2+}, Ba^{2+}, Pb^{2+}, Hg^{2+}, Ni^{2+}, and Cu^{2+} (10^{-3} mol L^{-1}), to a mixture containing buffered uranyl solution (5.0×10^{-3} mol L^{-1}). Under the optimized conditions, DPASV analysis was performed to compare the current response values of the blank solution before and after the addition of interfering metal ions. As shown in Fig. 7B, the electrochemical signals of the uranyl ions were not affected by the addition of interfering ions. Notably, the electrochemical DPASV signals of uranyl are not affected by the interfering species at a concentration of 150 fold of uranyl ions.

3.2.8. Analytical features. Under the optimized experimental conditions, as shown in Fig. 8, a wide linear range from 5×10^{-3} mol L^{-1} to 1×10^{-10} mol L^{-1} was observed using DPASV with a low limit of detection (2.1×10^{-11} mol L^{-1}). Good reproducibility (RSD = 2.1%) and intermediate precision (RSD = 2.7%) were observed for the MT/MWCNT/CPE sensor. To assess the stability of the proposed sensor, voltammetric measurements of the same solution were recorded and repeated for six weeks, and the data showed high stability, reaching 95% of the original values. Compared to other electrochemical techniques (Table 1), the proposed voltammetric sensor showed

Table 1 Different electrochemical techniques for UO_2^{2+} detection[a]

Method	Linear range (mol L^{-1})	Detection limit (mol L^{-1})	Quantification limit (mol L^{-1})	Stability (days)	Precision (RSD%)	Application	Ref.
DPAdSV	9.93×10^{-9}–2.64×10^{-7}	3.31×10^{-9}	—	5	5.03	Water	43
SV	7.94×10^{-9}–1.59×10^{-6}	9.93×10^{-10}	3.31×10^{-9}	15	5.4	Water	44
DPACSV	3.7×10^{-10}–3.7×10^{-8} 3.7×10^{-8}–3.7×10^{-5}	9.93×10^{-11}	3.31×10^{-10}	30	5.1	Water	45
AIEE	3.31×10^{-9} – 8.2×10^{-8}	6.62×10^{-10}	—	5	1.3	Water	46
DPASV	5×10^{-3}–1×10^{-10}	2.1×10^{-11}	7×10^{-11}	42	2.7	Water	This work

[a] Differential pulse adsorptive stripping voltammetry: DPAdSV; stripping voltammetry: SV; differential pulse adsorptive cathodic stripping voltammetry: DPACSV; aggregation-induced emission enhancement: AIEE; differential pulse anodic stripping voltammetry: DPASV.

Table 2 Determination of UO_2^{2+} in environmental water samples

Sample	Amount added ($\mu g\ L^{-1}$)	Amount found by DPASV ($\mu g\ L^{-1}$)	Recovery (%)
Sea water	0	1.7	—
	5	6.6	98.5
	10	11.65	99.5
Nile river water	0	4.0	—
	5	8.9	98.9
	10	14.0	100
Tap water	0	0.08	—
	5	5.04	99.2
	10	10.03	99.8

high sensitivity, good repeatability, excellent stability, and superb selectivity.

3.3. Analysis of UO_2^{2+} in actual water samples

To verify the feasibility and applicability of MT/MWCNT@CPE for the detection of uranyl ions in actual water samples, DPASV signals were recorded for each sample, and the concentration of UO_2^{2+} was determined based on the calibration curve; the output data are listed in Table 2. Furthermore, to evaluate the proposed technique, each sample was analyzed again *via* three parallel determinations using inductively coupled plasma-atomic emission spectroscopy (ICP-AES). The recovery percentage of UO_2^{2+} fell within the range of 97.8–99.3%, and the RSD values were lower than 4%. These results demonstrate that MT/MWCNT/CPE possesses proper accuracy and is applicable for the evaluation of uranyl ions in actual environmental samples.

4. Conclusions

A novel functionalized electrochemical sensor (MT/MWCNT/CPE) was fabricated by introducing melamine-thiourea-modified multiwalled carbon nanotubes (MT/MWCNT) into CPE components. Consequently, the selectivity and sensitivity of the proposed sensor toward uranyl ions were enhanced. In addition, the differential anodic stripping technique was used to detect uranyl ions over a wide range of concentrations from 5×10^{-3} to 1×10^{-10} mol L^{-1} with a low detection limit (2.1×10^{-11} mol L^{-1}). Furthermore, high repeatability, good reproducibility, and long-term stability (six weeks) were observed. Moreover, the modified sensor exhibited satisfactory results for the detection of uranyl ions in real water samples. Finally, the results of this study indicate that the developed sensor is an effective and useful platform for selective and rapid monitoring of UO_2^{2+} in the environment.

Data availability

The datasets used and/or analyzed during the current study are available from the corresponding author on reasonable request.

Author contributions

Fathi S. Awad, A. B. Abdallah, and Magdi E. Khalifa conceived the project, designed the experiments, analyzed the data, and wrote the paper. Amina A. Selim and Ahmed Fathi Salem Molouk prepared and characterized the samples, performed the experiments, analyzed the data, and drafted the manuscript. All authors read and approved the final form of the manuscript.

Conflicts of interest

There are no conflicts to declare.

Acknowledgements

References

1 J. Li and Y. Zhang, *Procedia Environ. Sci.*, 2012, **13**, 1609–1615.
2 J. L. Domingo, *Reprod. Toxicol.*, 2001, **15**, 603–609.
3 E. S. Craft, A. W. Abu-Qare, M. M. Flaherty, M. C. Garofolo, H. L. Rincavage and M. B. Abou-Donia, *J. Toxicol. Environ. Health, Part B*, 2004, **7**, 297–317.
4 M. Yazzie, S. L. Gamble, E. R. Civitello and D. M. Stearns, *Chem. Res. Toxicol.*, 2003, **16**, 524–530.
5 N. Goyal, P. J. Purohit, A. Dhobale, A. Page and M. Sastry, *Fresenius' Z. Anal. Chem.*, 1988, **330**, 114–115.
6 S. Abbasi, *Int. J. Environ. Anal. Chem.*, 1989, **36**, 163–172.
7 K. A. Stevenson, L. M. Blumberg and J. J. Harynuk, *Anal. Chim. Acta*, 2019, **1086**, 133–141.
8 D. Boomer and M. Powell, *Anal. Chem.*, 1987, **59**, 2810–2813.
9 A. Saha, K. Sanyal, N. Rawat, S. B. Deb, M. K. Saxena and B. S. Tomar, *Anal. Chem.*, 2017, **89**, 10422–10430.
10 K. Sanyal and N. Misra, *Spectrochim. Acta, Part B*, 2019, **155**, 44–49.
11 Z. Wang, D. Zhang, X. Xiao, C. Su, Z. Li, J. Xue, N. Hu, P. Peng, L. Liao and H. Wang, *Microchem. J.*, 2020, **155**, 104767.
12 S. Güney and O. Güney, *Sens. Actuators, B*, 2016, **231**, 45–53.
13 J. Tashkhourian, M. H. Nezhad, J. Khodavesi and S. Javadi, *J. Electroanal. Chem.*, 2009, **633**, 85–91.
14 M. Shamsipur, L. Samandari, L. Farzin and A. Besharati-Seidani, *Microchem. J.*, 2021, **160**, 105714.
15 J. Xue, C. Han, Y. Yang, S. Xu, Q. Li, H. Nie, J. Qian and Z. Yang, *Inorg. Chem.*, 2023, **62**, 3288–3296.
16 Y. Li, Z. Wang, C. Liu, D. Zhang, L. Liao and X. Xiao, *Z. Anorg. Allg. Chem.*, 2021, **647**, 1914–1920.
17 A. Kasaeinasab, H. A. Mahabadi, S. J. Shahtaheri, F. Faridbod, M. R. Ganjali and F. Mesgari, *PLoS One*, 2023, **18**, e0279816.
18 T. Liu, X. Zhang, B. Ke, Y. Wang, X. Wu, G. Jiang, T. Wu and G. Nie, *Mater. Sci. Eng., C*, 2016, **61**, 269–277.
19 H. Zhang, Y. Yuan, F. Yang, N. Zhang and X. Cao, *RSC Adv.*, 2015, **5**, 38630–38639.
20 M. A. Călin, L. R. Manea, L. Schacher, D. Adolphe, A. L. Leon, G. L. Potop and M. Agop, *J. Nanomater.*, 2015, **2015**, 6.

21 M. Rashid, T.-S. Jun, Y. Jung and Y. S. Kim, *Sens. Actuators, B*, 2015, **208**, 7–13.

22 H. Lai, P. Ming, M. Wu, S. Wang, D. Sun and H. Zhai, *Food Chem.*, 2023, **423**, 136331.

23 P. K. Kalambate, N. Larpant, R. P. Kalambate, W. Niamsi, V. Primpray, C. Karuwan and W. Laiwattanapaisal, *Sens. Actuators, B*, 2023, **378**, 133103.

24 P. K. Kalambate, M. R. Biradar, S. P. Karna and A. K. Srivastava, *J. Electroanal. Chem.*, 2015, **757**, 150–158.

25 X. Wang, A. Dong, Y. Hu, J. Qian and S. Huang, *Chem. Commun.*, 2020, **56**, 10809–10823.

26 W. Zhang, K. Shao, S. Li and Y. Xia, *J. Nucl. Radiochem.*, 1986, **8**, 102–107.

27 Y. Zhu, D. Zhang, F. Chang, J. Zhu, P. Wang, F. Tan, X. Li, L. Li and G. Hu, *Surf. Interfaces*, 2021, **25**, 101266.

28 X. Wu, Q. Huang, Y. Mao, X. Wang, Y. Wang, Q. Hu, H. Wang and X. Wang, *TrAC, Trends Anal. Chem.*, 2019, **118**, 89–111.

29 A. M. Bakry, F. S. Awad, J. A. Bobb, A. A. Ibrahim and M. S. El-Shall, *RSC Adv.*, 2020, **10**, 37883–37897.

30 A. M. El-Wakil, S. M. Waly, W. M. Abou El-Maaty, M. M. Waly, M. Yılmaz and F. S. Awad, *ACS Omega*, 2022, 7, 6058–6069.

31 X. Yuan, K. Luo, K. Zhang, J. He, Y. Zhao and D. Yu, *J. Phys. Chem. A*, 2016, **120**, 7427–7433.

32 H. Zhu and S.-a. Xu, *RSC Adv.*, 2018, **8**, 17879–17887.

33 S. Zhang, M. Zeng, W. Xu, J. Li, J. Li, J. Xu and X. Wang, *Dalton Trans.*, 2013, **42**, 7854–7858.

34 M. M. Gui, Y. X. Yap, S.-P. Chai and A. R. Mohamed, *Int. J. Greenhouse Gas Control*, 2013, **14**, 65–73.

35 M. S. Alhumaimess, *Sep. Sci. Technol.*, 2020, **55**, 1303–1316.

36 D. Vennerberg, R. Hall and M. R. Kessler, *Polymer*, 2014, **55**, 4156–4163.

37 F. S. Awad, K. M. AbouZied, W. M. Abou El-Maaty, A. M. El-Wakil and M. S. El-Shall, *Arabian J. Chem.*, 2020, **13**, 2659–2670.

38 F. S. Awad, K. M. AbouZeid, W. M. A. El-Maaty, A. M. El-Wakil and M. S. El-Shall, *ACS Appl. Mater. Interfaces*, 2017, **9**, 34230–34242.

39 R. Sitko, M. Musielak, M. Serda, E. Talik, B. Zawisza, A. Gagor and M. Malecka, *Sep. Purif. Technol.*, 2021, **254**, 117606.

40 N. M. Ghazy, E. A. Ghaith, Y. Abou El-Reash, R. R. Zaky, W. M. Abou El-Maaty and F. S. Awad, *RSC Adv.*, 2022, **12**, 35587–35597.

41 L. Jiang, S. Li, H. Yu, Z. Zou, X. Hou, F. Shen, C. Li and X. Yao, *Appl. Surf. Sci.*, 2016, **369**, 398–413.

42 P. Leuaa, D. Priyadarshani, D. Choudhury, R. Maurya and M. Neergat, *RSC Adv.*, 2020, **10**, 30887–30895.

43 Z. Zhou, Y. Zhou, X. Liang, F. Xie, S. Liu and J. Ma, *J. Radioanal. Nucl. Chem.*, 2019, **322**, 2049–2056.

44 S. Shi, H. Wu, L. Zhang, S. Wang, P. Xiong, Z. Qin, M. Chu and J. Liao, *J. Electroanal. Chem.*, 2021, **880**, 114884.

45 M. Kalate Bojdi, M. Behbahani, M. Najafi, A. Bagheri, F. Omidi and S. Salimi, *Electroanalysis*, 2015, **27**, 2458–2467.

46 X. Chen, L. He, Y. Wang, B. Liu and Y. Tang, *Anal. Chim. Acta*, 2014, **847**, 55–60.